

## Seismic performance of skewed highway bridges using analytical fragility function methodology

M. Bayat and F. Daneshjoo\*

*Department of Civil and Environmental Engineering, Tarbiat Modares University, Tehran, Iran*

*(Received October 23, 2015, Revised November 4, 2015, Accepted November 6, 2015)*

**Abstract.** In this study, the seismic performance of skewed highway bridges has been assessed by using fragility function methodology. Incremental Dynamic Analysis (IDA) has been used to prepare complete information about the different damage states of a 30 degree skewed highway bridge. A three dimensional model of a skewed highway bridge is presented and incremental dynamic analysis has been applied. The details of the full nonlinear procedures have also been presented. Different spectral intensity measures are studied and the effects of the period on the fragility curves are shown in different figures. The efficiency, practicality and proficiency of these different spectral intensity measures are compared. A suite of 20 earthquake ground motions are considered for nonlinear time history analysis. It has been shown that, considering different intensity measures (IM) leads us to overestimate or low estimate the damage probability which has been discussed completely.

**Keywords:** nonlinear time history analysis; fragility function methodology; intensity measures

---

### 1. Introduction

In recent years, seismic vulnerability of skewed highway bridges has become more important especially after the damage caused by the San Fernando earthquake (1971). When the skew degree increases the behavior becomes complex and the effects of coupling becomes more important. In fact, the seismic vulnerability of skewed highway bridges is greater than straight highway bridges. In the last few decades many researchers have studied the seismic responses of skewed highway bridges; however the research findings have not been comprehensive enough to address global system response. Design codes and guidelines have improved significantly for dynamic and static analyses of straight highway bridges. However, the lack of detailed procedure is still seen for the responses of skewed highway bridges.

Some important skewed bridges which have failed during earthquakes had large skew angles such as: Foothill Boulevard Undercrossing bridge with a 60 degree skew under San Fernando earthquake in 1971, Gavin Canyon Undercrossing with a 66 degree skew under Northridge earthquake in 1994 and etc.

Ghobarah and Tso (1973) studied the behavior of the Foothill skewed bridge in 1974. In this

---

\*Corresponding author, Professor, E-mail: [danesh\\_fa@modares.ac.ir](mailto:danesh_fa@modares.ac.ir)  
M. Bayat, E-mail: [mbayat14@yahoo.com](mailto:mbayat14@yahoo.com)

study the bridge was modeled by a flexible beam fixed at both ends in abutments. Torsional and flexural modes with out of plane deformations were considered for it. The bridge was analyzed under the vertical component force of the San Fernando earthquake and it was concluded that damage was caused by Torsional and flexural movements of the deck and because of the out of plane movements, bases were disjointed under heavy pressure. Maragakis and Jenings (1987) studied the damage and aftermath of the 1971 San Fernando earthquake on California bridges. They concluded that in most cases in skewed highway bridges, damage was caused by the movement of the rigid body of deck accompanied by consecutive impacts of deck and side supports, which in turn were cause by dynamic vibrations of the bridge. In that study it was mentioned that overpass and underpass bridges of Foot Hill Boulevard and overpass bridge of San Fernando have the same condition.

The simple model was devised to identify the main parameters in analyzing the bridge's behavior, and the complicated model which is more detailed was devised to examine the effect of these parameters on bridge's behavior. The complicated model was used to analyze the rigid body of Nicols's overpass skewed bridge (with 20 degree angle) located in Riverside California. Wikfield *et al.* (1991) used two Finite Element Models to analyze the Foothill skewed bridge, assuming linear and nonlinear behavior for the columns. The difference of the two models was in modeling the deck. In the first model the deck was modeled using bar's element and in the second model the deck was modeled using shell elements. The second model was more accurate and yielded a more realistic behavior of the bridge's response. In dynamic linear and nonlinear analysis of the transverse component of an earthquake the second model was used.

Mang and Luie (2002) in a similar study used three finite element models to analyze the skewed bridge of Foot hill under the effect of modified longitudinal transversal and vertical components of the earthquake (1971) using the spectral method and assuming the linear behavior of bases. Three models were devised. In two of the models the deck was modeled using a shell element as elastic and rigid, and for the third model the deck was modeled using a beam-column element as a stick model. Free vibration analysis was performed to determine the natural periods and mode shapes using these three models. The assumption of this study was similar to Wikfield *et al.* (1991) except that in this study the rotation of nodes in side abutments along the longitudinal axis was disregarded. The results of free vibration analysis of the three models shows that in all three cases, the rotation mode of the deck in the plane was vertical rotation and in the second and third models the movements of the stick model and the rigid deck model were only transmission motion, but in these two modes the elastic deck model experienced motion transmission as well as torsion and bending movements.

In considering the research from an accuracy point of view, Shinozuka *et al.* (2001) represented an essay on fragility curves that in comparison to previous works was more accurate. This essay represented the fragility curves for common bridges in southern California which had concrete columns and were retrofitted with metallic coating. The high accuracy of this research owes to the statistical method of software and the use of the dynamic technique of the nonlinear method and for the first time showed that the fragility curve is statistical if used for considering accuracy. Shinozuka *et al.* (2002) developed the same procedure for multi-span concrete bridges. In this study the historical records were used for dynamic analysis and the fragility curves were in two states: it's supposed that bridge was symmetric and all the columns were on the same type of soil).

Following these works, Mackie and Stojadinovic (2003) extracted fragility curves for highway bridges of California. Using the methods of earthquake classification which was explained above they extracted the desired accelerograms and defined different criteria of applied earthquakes.

Shahria Alam *et al.* (2012) performed an analytical study in 2012 on fragility curves of a three span bridge with a continuous deck with seismic isolation installed and with shape-memory alloys. Fragility function was defined in Siesmo Struct. Incremental dynamic analysis was performed using record with PGA between 0.4 g and 1.07 g. In this study two types of rubber seats were used in bridges, one with high damping and another with lead core in addition to tying made of shape-memory alloy. Fragility curves were extracted for one of the bases, one of the isolators and the whole system. Fragility curves of bridges were used to assess the bridge's system in deferent levels of damage. From the numerical results it can be concluded that on average PGAs different levels of damage are lower in systems with SMA compared to systems without SMA. Also, in bridges with seismic isolation damage is more concentrated on the separators rather than the piers of the bridge.

There are other related papers on the seismic vulnerability of bridges and fragility assessment procedures of structures available. Ataei and Padgett (2013), Cimerallo *et al.* (2010), Bisadi *et al.* (2011), Choi (2002), Deepu *et al.* (2014), Eads *et al.* (2013), Elnashai and Borzi (2004), Kameshwar and Padgett (2014), Katsanos and Sextos (2013), Padgett *et al.* (2008), Sung and Su (2011), Tavares *et al.* (2012), Wright *et al.* (2011), Yi *et al.* (2007), Bayat *et al.* (2015a, b), Kalantari and Amjadian (2010), Amjadian and Kalantari (2012).

Fragility curves can be divided into two categories: (a) Empirical fragility curves, (b) analytical fragility curves. In this study, we have considered the analytical fragility curves of skewed highway bridges using different intensity measures (IMs). A more complete overview of these two approaches has been published in previous papers. In this paper an Incremental dynamic analysis (IDA) has been used to develop the fragility curves of a 30 degree skewed bridge by considering the effect of different spectral intensity measures on its seismic response. A detailed three dimensional model of the bridge has been presented. A full nonlinear time history analysis is utilized to evaluate the seismic response of bridge components (bridge piers).

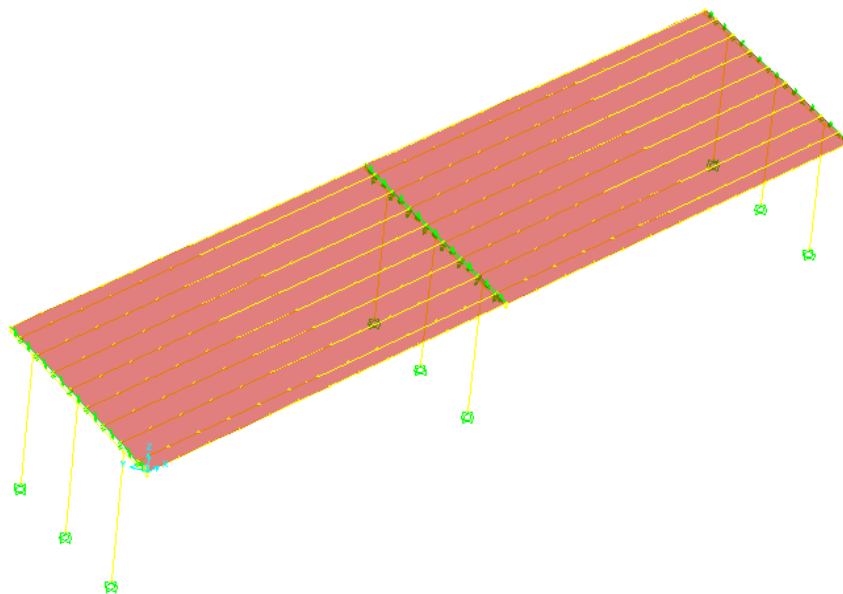


Fig. 1 Three dimensional model of the 30 skewed bridge in SAP2000

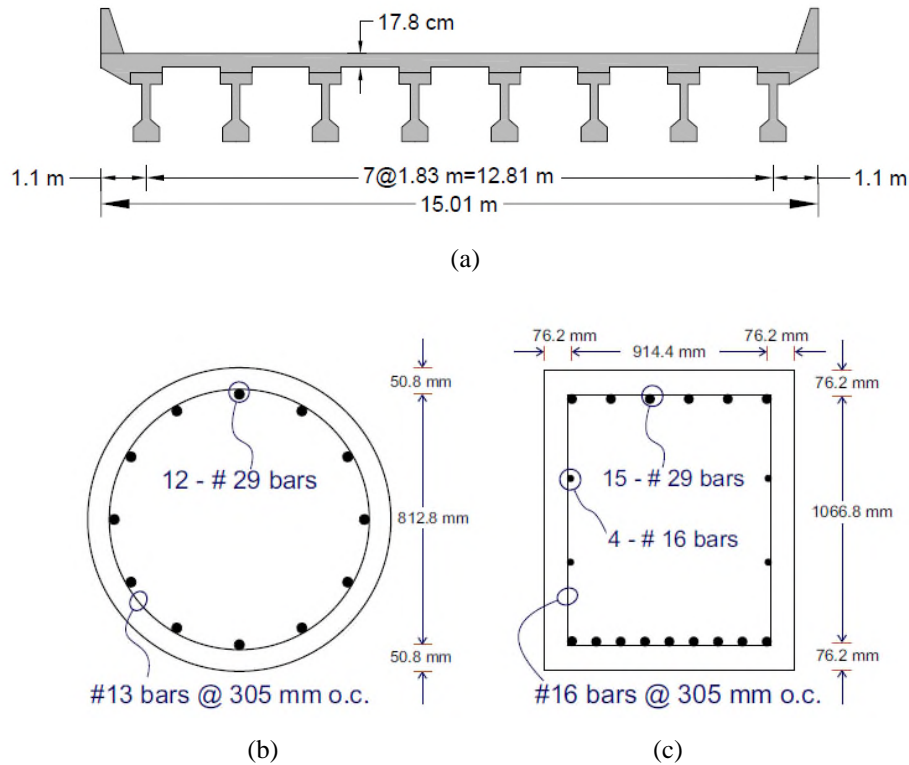


Fig. 2 Concrete member reinforcing layout: (a) Deck detail; (b) Column; (c) Bent beam

## 2. Bridge configurations and modeling

The model used in this study is derived from a non-skewed model developed by Nielson (2005) the characteristics of which are based on data obtained from a survey of numerous bridge plans. Total length of the bridge is 48.8 m and its two equal spans have 24.4 m length. The width of bridge is 15.01 m with eight AASHTO type prestressed girders. AASHTO Type I and III girders are used for the end and centre spans. Elastomeric pads are the bearing of this bridge. The pads for end spans are 406 mm long by 152 mm wide and 25.4 mm thick and for the centre span which are 559 mm long by 203 mm wide and still 25.4 mm thick. The concrete strength of the design is assumed to be 20.7 MPa while the yield strength of reinforcing steel is 414 MPa. More detailed specifications of these columns are in an investigation of existing bridge plans and also from the work done by Hwang *et al.* (2001). Fig. 1 shows a three dimensional model of the considered bridge and the detail of the column and deck and cap beam are presented in Fig. 2. The deck is modelled using shell elements. The abutments are modelled using beam elements supported on springs. A rigid bar is used to connect the nodes between girders and bearings, bearings and cap beams, and cap beams and tops of the columns. Abutments and the column boundary conditions are fixed-free in the longitudinal direction and fixed-fixed in the transverse direction.

### 3. Fragility function methodology

Cornell *et al.* (2002) formulated the procedure of developing the analytical fragility functions. The fragility curves are the relation between the seismic hazard and response of structures and modeled as lognormal distribution Cornell *et al.* (2002)

$$P[D \geq d | IM] = 1 - \phi \left( \frac{\ln(d) - \ln(S_D)}{\beta_{D|IM}} \right) \quad (1)$$

$\phi(\bullet)$  = Standard normal cumulative distribution function

$S_D$  = Median value of the structural demand in terms of a seismic intensity

$\beta_{D|IM}$  =Logarithmic standard deviation, or dispersion, of the demand conditioned on the IM.

The relation between SD and IM estimated as

$$S_D = aIM^b \quad (2)$$

With a linear regression we can obtain the coefficient of a and b and re-written the Eq. (2) as

$$\ln(SD) = b \cdot \ln(IM) + \ln(a) \quad (3)$$

The dispersion of the mean demand conditioned on the IM is

$$\beta_{D|IM} \cong \sqrt{\frac{\sum (\ln(d_i) - \ln(b \cdot \ln(IM) + \ln(a)))^2}{N - 2}} \quad (4)$$

$N$ = number of ground motions

$d_i$  = Peak demands

#### 3.1 Efficient intensity measure

If an IM is efficient it should have a less dispersion about the median of the results of nonlinear time history analysis.  $\beta_{D|IM}$  is the dispersion of the results around the median of the response in this study. The lower values of  $\beta_{D|IM}$  leads to a more efficient intensity measure Padgett *et al.* (2008).

#### 3.2 Practical intensity measure

Padgett *et al.* (2008) presented a new criteria of selecting an optimal intensity measure in bridges. They introduce the practicality of an intensity measure which is the relation between the dependency of the structural response and seismic hazard. They identified the practicality as a coefficient of the regression parameter  $b$  in Eq. (3). The higher value of  $b$  leads to a more practical intensity measure in comparison together.

#### 3.3 Proficient intensity measure

Padgett *et al.* (2008) composite the measure of efficiency and practicality as new criteria of

selecting an optimal intensity measure as follow formulation

$$P[D \geq d | IM ] = 1 - \phi \left( \frac{\ln(IM) - \frac{\ln(d) - \ln(a)}{b}}{\frac{\beta_{D|IM}}{b}} \right) \tag{5}$$

A lower values of modified dispersion is a more proficient IM

$$\zeta = \frac{\beta_{D|IM}}{b} \tag{6}$$

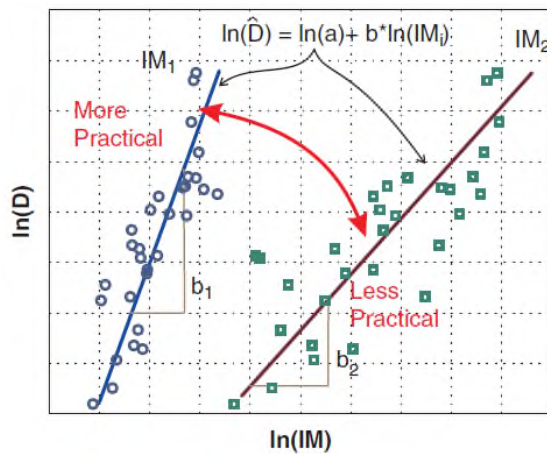


Fig. 3 Graphical meaning of the *b* parameter Padgett *et al.* (2008)

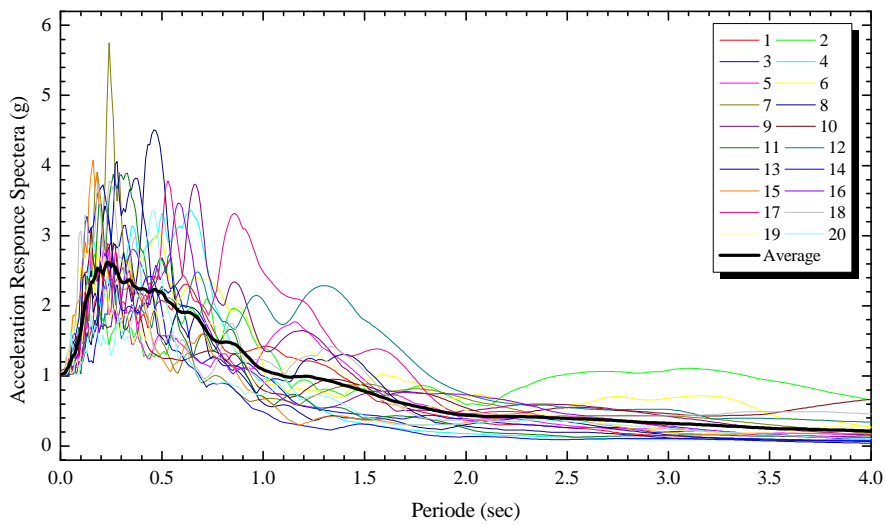


Fig. 4 Response acceleration spectra of far field ground motions

Table 1 Characteristics of the earthquake ground motion histories FEMA (2003)

ID No	M	PGA (g)	Year	Earthquake		Recording station	
				Name	Name	owner	
1	7.0	0.48	1992	Cape Mendocino	Rio Dell Overpass	USGS	
2	7.6	0.21	1999	Chi-Chi, Taiwan	CHY101	CWB	
3	7.1	0.82	1999	Duzce, Turkey	Bolu	ERD	
4	6.5	0.45	1976	Friuli, Italy	Tolmezzo	-----	
5	7.1	0.35	1999	Hector Mine	Hector	SCSN	
6	6.5	0.34	1979	Imperial Valley	Delt	UNAMUCSD	
7	6.5	0.35	1979	Imperial Valley	El Centro Array#1	USGS	
8	6.9	0.38	1995	Kobe, Japan	Nishi-Akashi	CUE	
9	6.9	0.51	1995	Kobe, Japan	Shin-Osaka	CUE	
10	7.5	0.24	1999	Kokaeli, Turkey	Duzce	ERD	
11	7.3	0.36	1992	Landers	Yemo Fire Station	CDMG	
12	7.3	0.24	1992	Landers	Coolwater	SCE	
13	6.9	0.42	1989	Loma Prieta	Capitola	CDMG	
14	6.9	0.53	1989	Loma Prieta	Gilory Arrey#3	CDMG	
15	7.4	0.56	1990	Manjil	Abbar	BHRC	
16	6.7	0.55	1994	Northridge	Beverly Hills-Mulhol	USC	
17	6.7	0.44	1994	Northridge	Canyon Country-WLC	USC	
18	6.6	0.36	1971	San Ferando	LA-Hollywood Stor	CDMG	
19	6.5	0.51	1987	Superstition Hills	El Centro Imp.Co	CDMG	
20	6.5	0.52	1987	Superstition Hills	Poe Road (temp)	USGS	

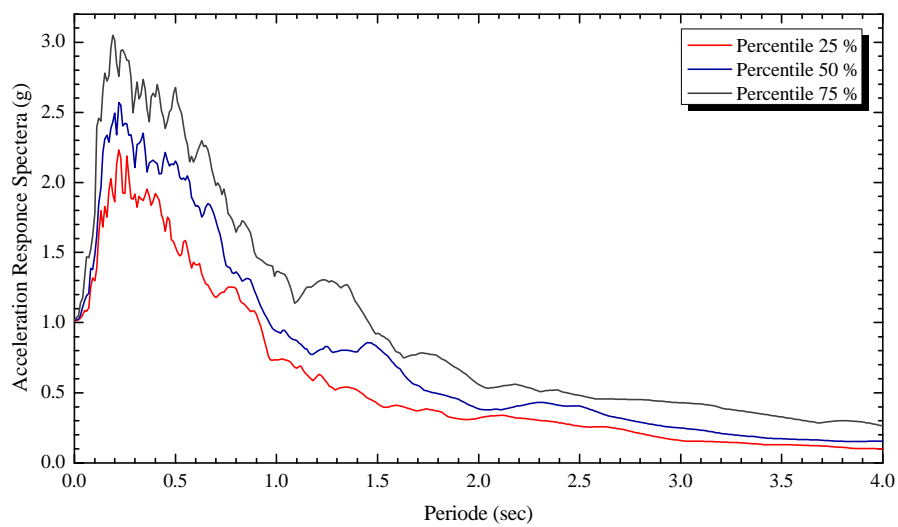


Fig. 5 Percentiles of response acceleration spectra of a suit of 20 far field earthquake ground motion records

#### 4. Selection of ground motion

Twenty earthquake ground motions have been selected for incremental dynamic analysis. A general far-field ground motions set (see Table 1) is developed, based on FEMA-P695 far field ground motion records FEMA (2003): The FEMA records satisfy the following criteria

(a) Magnitude  $> 6.5$ ; (b) Distance from source to site  $> 10$  km (average of Joyner-Boore and Campbell distances) Joyner and Boore (1993); (c) Peak Ground Acceleration (PGA)  $> 0.2$  g and Peak Ground Velocity (PGV)  $> 15$  cm/sec; (d) Soil shear wave velocity, in the upper 30 m, greater than 180 m/s; (e) Lowest useable frequency  $< 0.25$  Hz, to ensure that the low frequency content was not removed by the ground motion filtering process; (f) Strike-slip and thrust faults (consistent with California); (g) No consideration of spectral shape; (h) No consideration of station housing, but PEER-NGA records were selected to be “free-field”.

Figs. 4 and 5 represent the average spectrum of the records and different percentiles of acceleration response spectra with 5% damping ratio.

#### 5. Incremental Dynamic Analysis (IDA)

Incremental dynamic analysis (IDA) has been used to develop the analytical fragility curves in this study. The records were scaled up to the maximum considered PGA, stopping the scaling if the extensive limit state is reached ( $PGA_{max}=2$  g). IDA prepares valuable information of the elastic behavior of the structure till the nonlinear. The suite of records (at least 20) is scaled to different intensity levels with the increment of 0.1 (FEMA 2003). For each record the dynamic analysis was run and the results post-processed.

#### 6. Characterization of damage states

Different Engineering Demand Parameters (EDP) for highway bridges which have been presented in Table 2. In this study, column drift ratio has been assumed as EDP, and evaluated it considering the combination of transverse and longitudinal displacements

Table 2 Summary of DIs and corresponding LS for concrete columns

Bridge component	DS	Slight (DS=1)	Moderate (DS=2)	Extensive (DS=3)	Collapse (DS=4)
Column	A Physical phenomenon	Cracking and spalling	Moderate cracking and spalling	Degradation without collapse	Failure leading to collapse
	B Section ductility $\mu_k$	$\mu_k > 1$	$\mu_k > 2$	$\mu_k > 4$	$\mu_k > 7$
	C Drift ratio	$\theta > 0.007$	$\theta > 0.015$	$\theta > 0.025$	$\theta > 0.05$

A. HAZUZ (1999); B. Choi *et al.* (2004); C. Yi *et al.* (2007)

#### 7. Results and discussions

In this section, graphs and a table are presented to show a complete comparison between

different intensity measures. Some criteria for finding the optimal intensity measure was presented in previous sections. Efficiency and practicality and proficiency of an intensity measure were shown in Eqs. (4) and (6). The  $\beta_{EDP|IM}$  shows the dispersion of the results in linear regression in logarithmic space, the less value of  $\beta_{EDP|IM}$  leads us to more efficient intensity measure. The value shown is the practicality of an intensity measure, the high values of  $b$  leads us to more practical intensity measure.

A composite criterion has been presented as  $\zeta = \frac{\beta_{EDP|IM}}{b}$ . The lower values of  $\zeta$  leads us to more efficient and more practical intensity measure. Fig. 6 represents the results of incremental

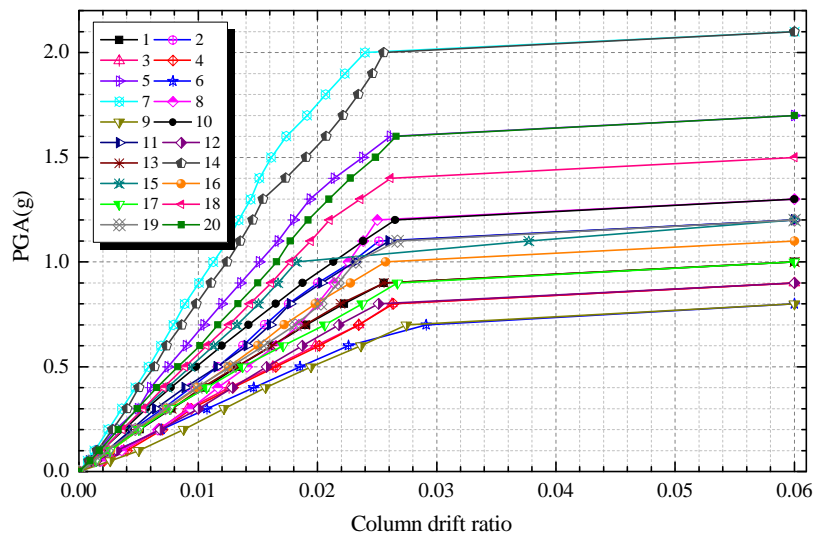


Fig. 6 IDA curves: 30 degree skewed highway bridge corresponding to the set of selected accelerograms IM=PGA, EDP= $\theta_{max}$

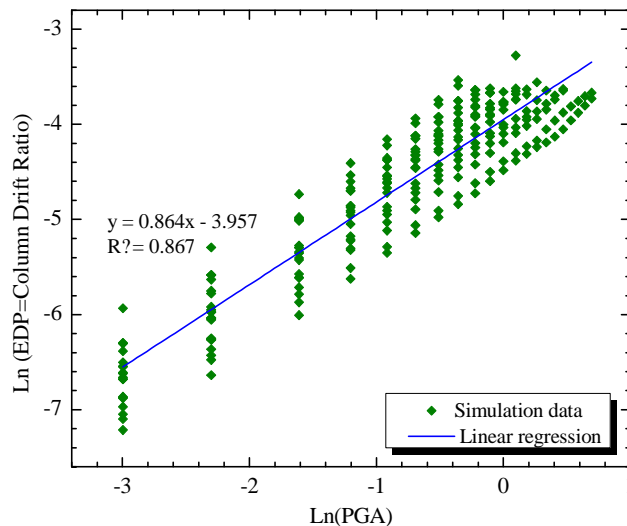


Fig. 7 Simulated maximum column drift ratio (as EDP) of bridge as a function of PGA (as IM) of earthquake motions

dynamic analysis, the selected intensity measure is PGA and the selected engineering demand parameter is column drift ratio. The complete comparison for the different spectral intensity measures and PGA are presented in Table 3. The trend of the selection of an intensity measure with respect to the efficiency, practicality and proficiency have been shown. The Sa(1.1Ts,5%) is the optimal spectral intensity measure. It is followed by Sa(Ts,5%) and Sa(1.2Ts,5%). There is a difference of greater than 80% between the selected optimal intensity measure and the PGA which is more than 80%. Figs. 7 to 23 show the results of linear regression analysis of the nonlinear time history analysis and also the efficiency and practicality of the intensity measures. The practicality of the intensity measures is clearer when considering the figures in detail. To have a better understanding of the effects of the different intensity measure of the failure probability of the

Table 3 Comparisons of regression values of PGA and Sa (Ti,5%) and dispersion values

IM	Ln (a)	<i>b</i>	$\beta_{EDP IM}$	$\zeta = \frac{\beta_{EDP IM}}{b}$	Differences (%)
<b>PGA(g)</b>	<b>-3.95</b>	<b>0.864</b>	<b>1.240</b>	<b>1.435</b>	<b>89.564</b>
Sa(0.1Ts,5%)	-4.18	0.826	2.107	2.550	236.856
Sa(0.2Ts,5%)	-4.6	0.778	1.608	2.067	173.052
Sa(0.3Ts,5%)	-4.73	0.728	1.815	2.493	229.326
Sa(0.4Ts,5%)	-4.75	0.74	1.780	2.405	217.701
Sa(0.5Ts,5%)	-4.65	0.846	1.341	1.585	109.379
Sa(0.6Ts,5%)	-4.6	0.858	1.249	1.456	92.338
Sa(0.7Ts,5%)	-4.59	0.809	1.412	1.746	130.647
Sa(0.8Ts,5%)	-4.48	0.888	1.125	1.267	67.371
Sa(0.9Ts,5%)	-4.39	0.928	1.122	1.210	59.841
<b>Sa(Ts,5%)</b>	<b>-4.34</b>	<b>0.932</b>	<b>0.769</b>	<b>0.825</b>	<b>8.983</b>
<b>Sa(1.1Ts,5%)</b>	<b>-4.22</b>	<b>0.944</b>	<b>0.714</b>	<b>0.757</b>	<b>0.000</b>
<b>Sa(1.2Ts,5%)</b>	<b>-4.17</b>	<b>0.92</b>	<b>0.864</b>	<b>0.939</b>	<b>24.042</b>
Sa(1.3Ts,5%)	-4.14	0.895	1.068	1.193	57.596
Sa(1.4Ts,5%)	-4	0.902	1.005	1.114	47.160
Sa(1.5Ts,5%)	-3.9	0.853	1.292	1.515	100.132
Sa(1.6Ts,5%)	-3.9	0.813	1.470	1.808	138.838
Sa(1.7Ts,5%)	-3.89	0.772	1.616	2.094	176.618
Sa(1.8Ts,5%)	-3.89	0.734	1.757	2.394	216.248
Sa(1.9Ts,5%)	-3.9	0.708	1.854	2.618	245.839
Sa(2Ts,5%)	-3.89	0.706	1.863	2.639	248.613
Sa(2.1Ts,5%)	-3.8	0.712	1.862	2.615	245.443
Sa(2.2Ts,5%)	-3.8	0.729	1.801	2.470	226.288
Sa(2.3Ts,5%)	-3.7	0.732	1.795	2.452	223.910
Sa(2.4Ts,5%)	-3.6	0.744	1.764	2.371	213.210
Sa(2.5Ts,5%)	-3.6	0.741	1.766	2.383	214.795

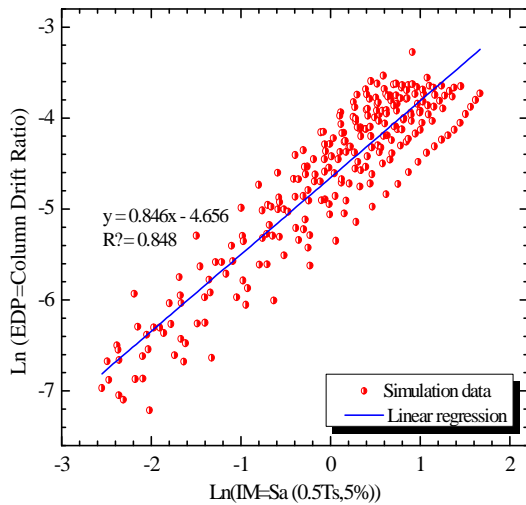


Fig. 8 Simulated maximum column drift ratio (as EDP) of bridge as a function of Sa(0.5Ts,5%) (as IM) of earthquake motions

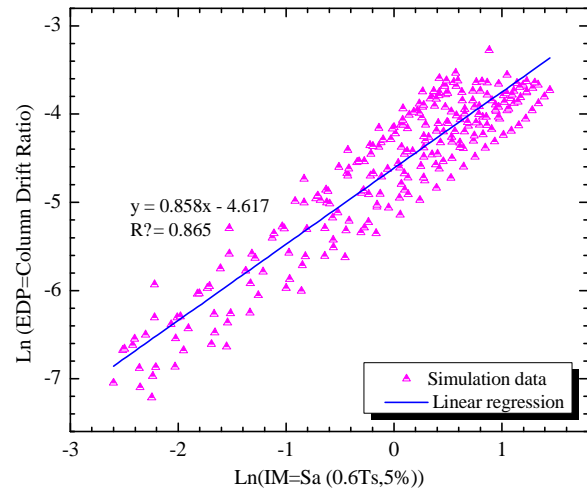


Fig. 9 Simulated maximum column drift ratio (as EDP) of bridge as a function of Sa(0.6Ts,5%) (as IM) of earthquake motions

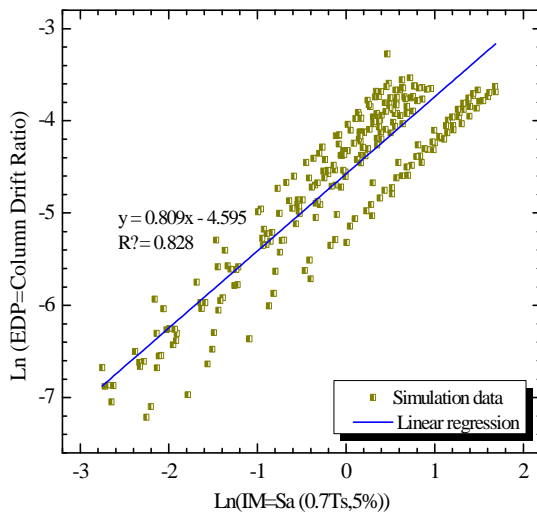


Fig. 10 Simulated maximum column drift ratio (as EDP) of bridge as a function of Sa(0.7Ts,5%) (as IM) of earthquake motions

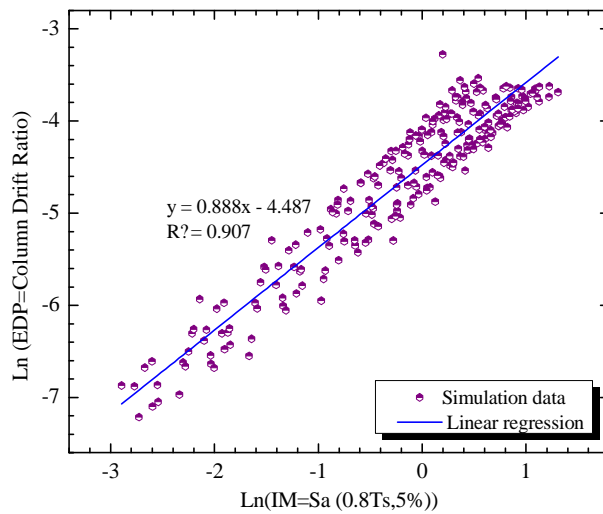


Fig. 11 Simulated maximum column drift ratio (as EDP) of bridge as a function of Sa(0.8Ts,5%) (as IM) of earthquake motions

bridge, we have considered the different fragility curves to show these differences.

Figs. 24 to 40 show the results of the fragility curves with respect to these 26 intensity measures. With careful attention to these results, it has been shown that choosing different intensity measures leads us to overestimate or low estimate the failure probability of the structure. The comparison should be done between the optimal spectral intensity measure and the other spectral intensity measures that follow.

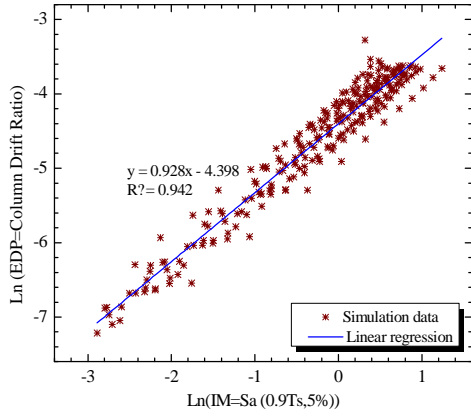


Fig. 12 Simulated maximum column drift ratio (as EDP) of bridge as a function of Sa(0.9Ts,5%) (as IM) of earthquake motions

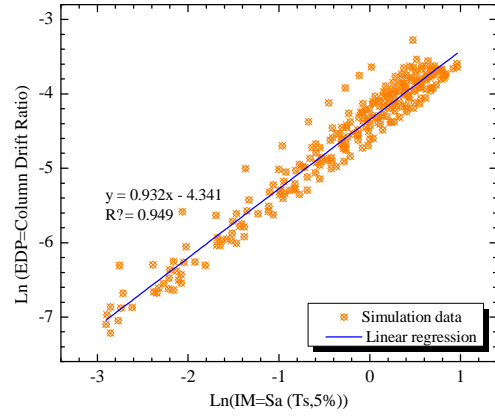


Fig. 13 Simulated maximum column drift ratio (as EDP) of bridge as a function of Sa(Ts,5%) (as IM) of earthquake motions

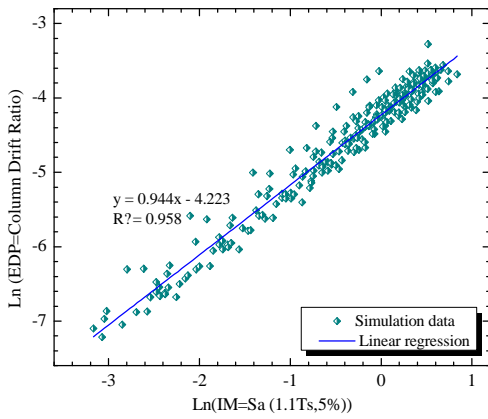


Fig. 14 Simulated maximum column drift ratio (as EDP) of bridge as a function of Sa(1.1Ts,5%) (as IM) of earthquake motions

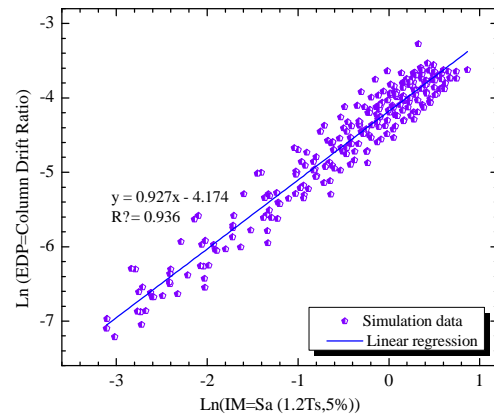


Fig. 15 Simulated maximum column drift ratio (as EDP) of bridge as a function of Sa(1.2Ts,5%) (as IM) of earthquake motions

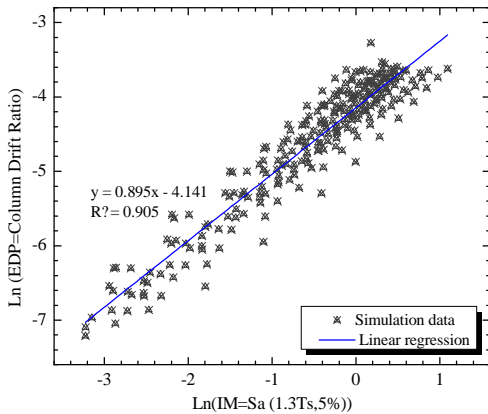


Fig. 16 Simulated maximum column drift ratio (as EDP) of bridge as a function of Sa(1.3Ts,5%) (as IM) of earthquake motions

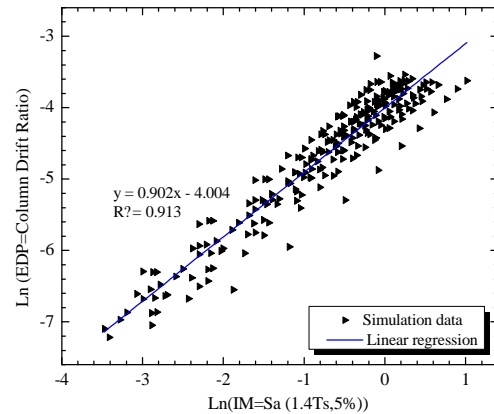


Fig. 17 Simulated maximum column drift ratio (as EDP) of bridge as a function of Sa(1.4Ts,5%) (as IM) of earthquake motions

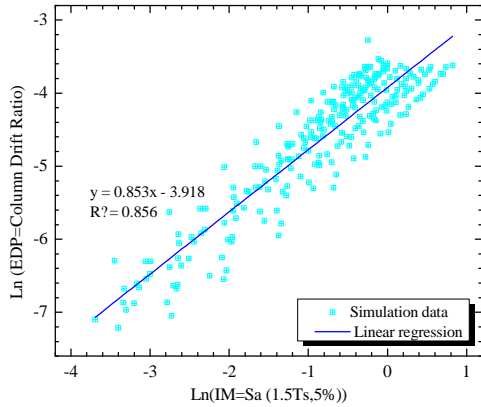


Fig. 18 Simulated maximum column drift ratio (as EDP) of bridge as a function of Sa(1.5Ts,5%) (as IM) of earthquake motions

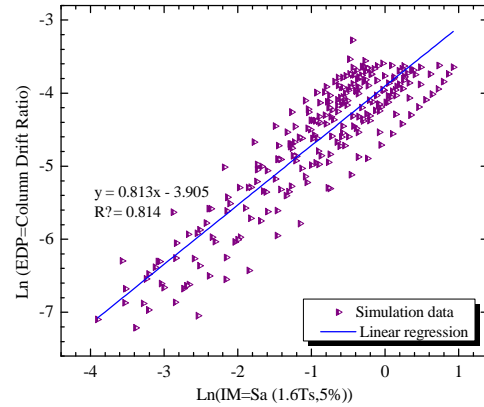


Fig. 19 Simulated maximum column drift ratio (as EDP) of bridge as a function of Sa(1.6Ts,5%) (as IM) of earthquake motions

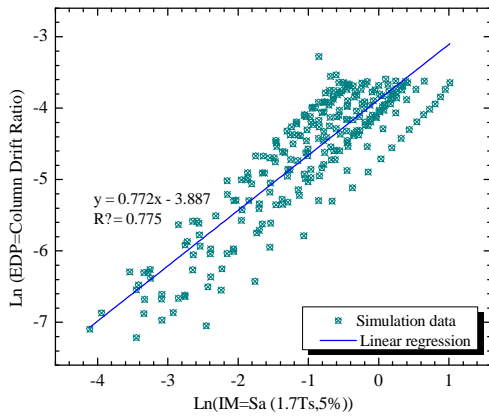


Fig. 20 Simulated maximum column drift ratio (as EDP) of bridge as a function of Sa(1.7Ts,5%) (as IM) of earthquake motions

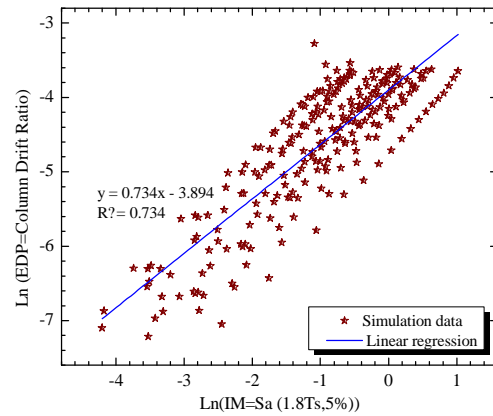


Fig. 21 Simulated maximum column drift ratio (as EDP) of bridge as a function of Sa(1.8Ts,5%) (as IM) of earthquake motions

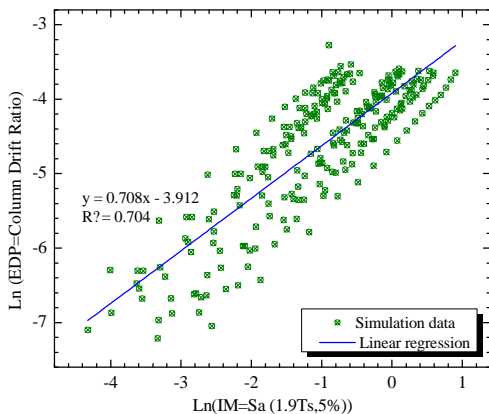


Fig. 22 Simulated maximum column drift ratio (as EDP) of bridge as a function of Sa(1.9Ts,5%) (as IM) of earthquake motions

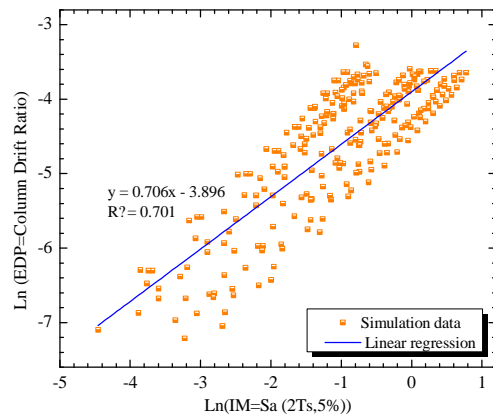


Fig. 23 Simulated maximum column drift ratio (as EDP) of bridge as a function of Sa(2Ts,5%) (as IM) of earthquake motions

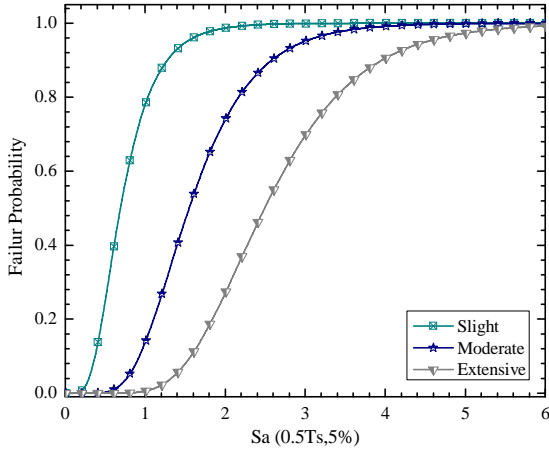


Fig. 25 Fragility curves of the bridge pier respect to  $Sa(0.5 T_s, 5\%)$

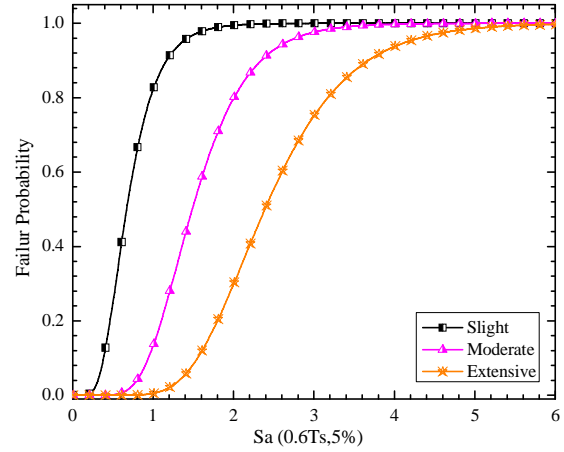


Fig. 26 Fragility curves of the bridge pier respect to  $Sa(0.6 T_s, 5\%)$

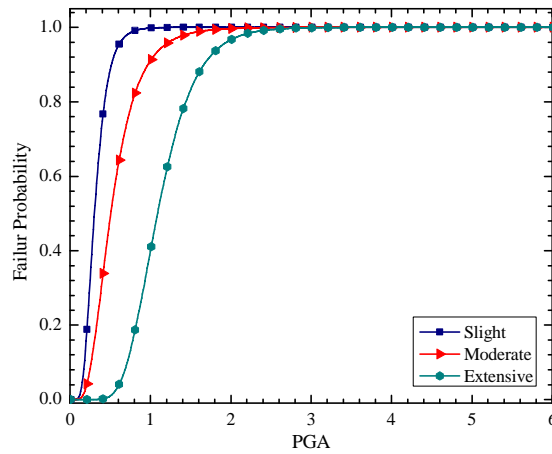


Fig. 24 Fragility curves of the bridge pier respect to PGA

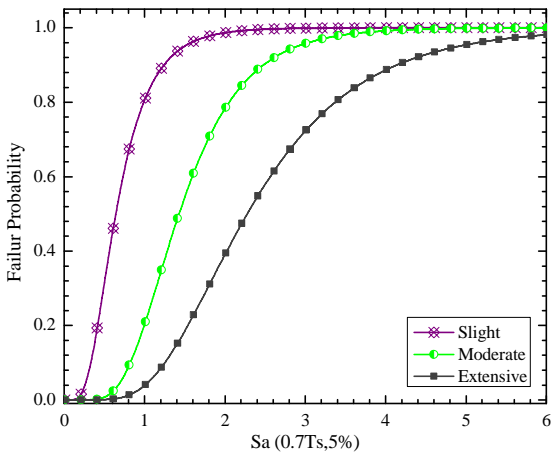


Fig. 27 Fragility curves of the bridge pier respect to  $Sa(0.7 T_s, 5\%)$

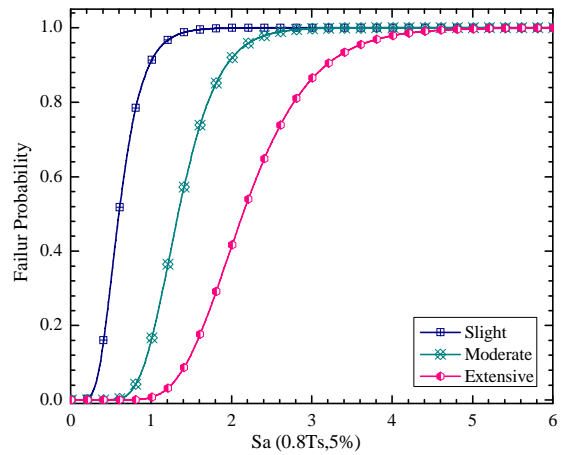


Fig. 28 Fragility curves of the bridge pier respect to  $Sa(0.8 T_s, 5\%)$

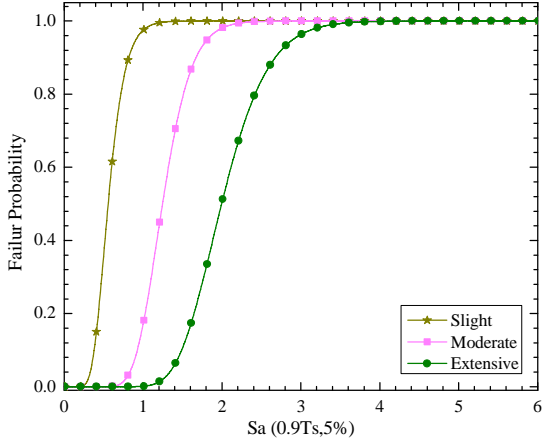


Fig. 29 Fragility curves of the bridge pier respect to  $Sa(0.9 T_s, 5\%)$

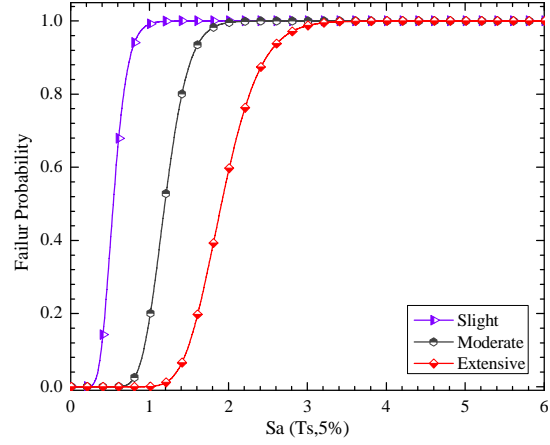


Fig. 30 Fragility curves of the bridge pier respect to  $Sa(T_s, 5\%)$

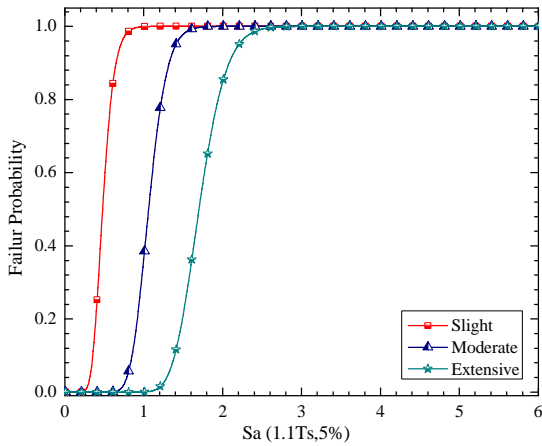


Fig. 31 Fragility curves of the bridge pier respect to  $Sa(1.1 T_s, 5\%)$

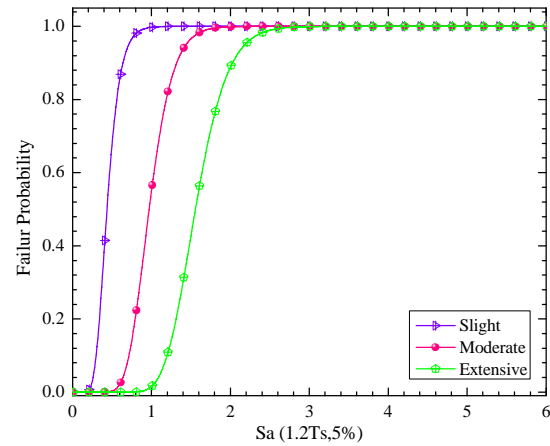


Fig. 32 Fragility curves of the bridge pier respect to  $Sa(1.2 T_s, 5\%)$

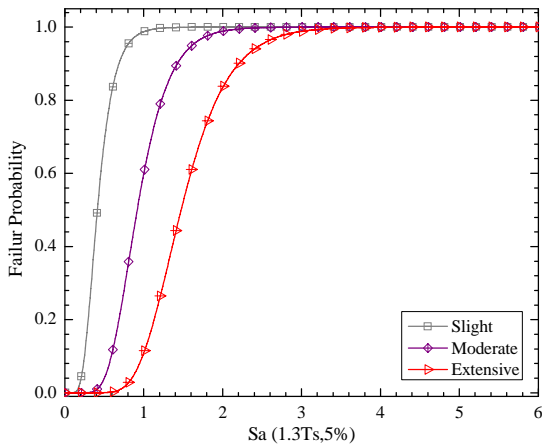


Fig. 33 Fragility curves of the bridge pier respect to  $Sa(1.3 T_s, 5\%)$

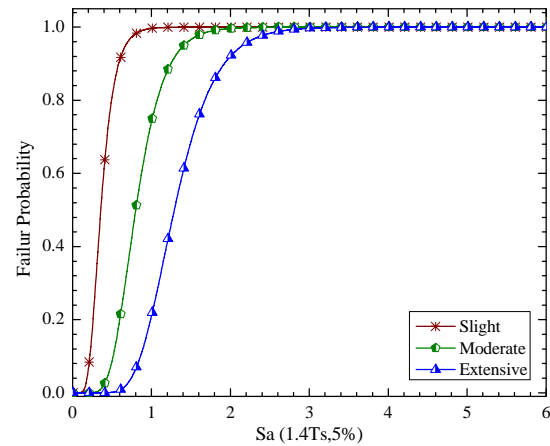


Fig. 34 Fragility curves of the bridge pier respect to  $Sa(1.4 T_s, 5\%)$

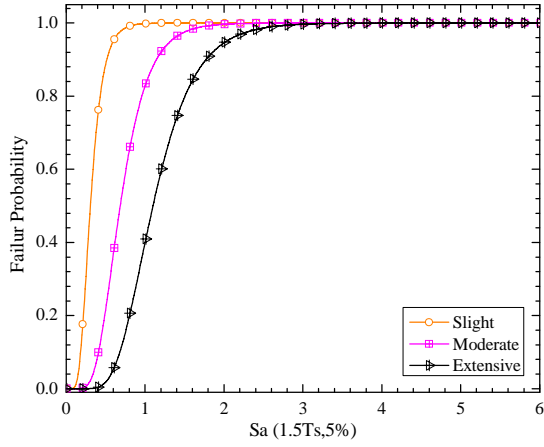


Fig. 35 Fragility curves of the bridge pier respect to Sa (1.5Ts,5%)

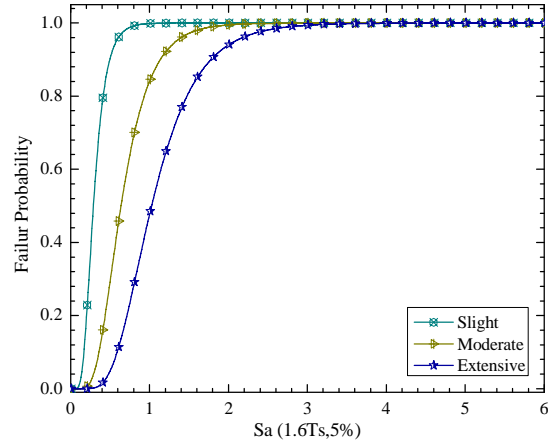


Fig. 36 Fragility curves of the bridge pier respect to Sa (1.6 Ts,5%)

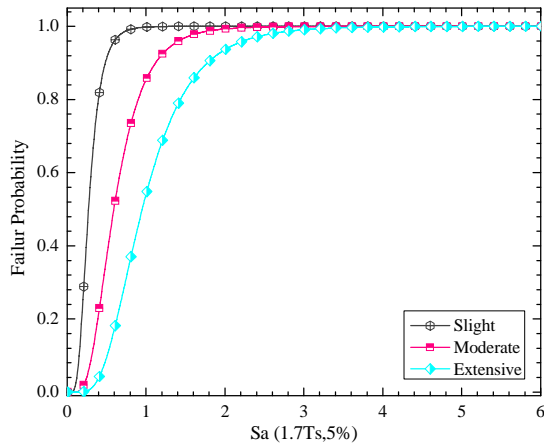


Fig. 37 Fragility curves of the bridge pier respect to Sa(1.7 Ts,5%)

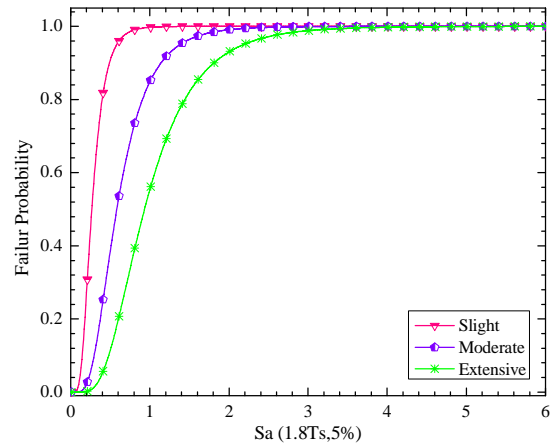


Fig. 38 Fragility curves of the bridge pier respect to Sa(1.8 Ts,5%)

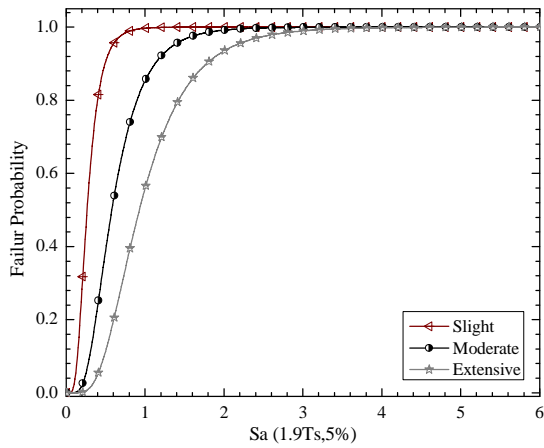


Fig. 39 Fragility curves of the bridge pier respect to Sa(1.9 Ts,5%)

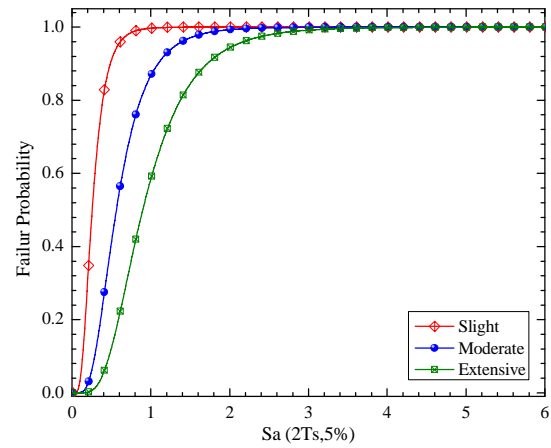


Fig. 40 Fragility curves of the bridge pier respect to Sa (2 Ts,5%)

## 8. Conclusions

In this study, the focus has been on the seismic analytical fragility curve of the skewed highway bridge. A 30 skew degree bridge is studied in detail. Different spectral intensity measures from  $S_a(0.5T_s, 5\%)$  to  $S_a(2.5T_s, 5\%)$  are studied completely. The efficiency, practicality and proficiency were considered in tables and figures. It has been shown that selection of an optimal intensity measure will lead us to more high accurate fragility curves. The spectral intensity measure leads us to more accurate results compared to PGA in our study for a skew highway bridge.

## References

- Agency, F.E.M. (2009), "Quantification of building seismic performance factors", FEMA P695, Washington, DC.
- Alam, S., Rahman Bhuiyan, M.A. and Muntasir Billah, A.H.M. (2012), "Seismic fragility assessment of SMA-bar restrained multi-span continuous highway bridge isolated by different laminated rubber bearings in medium to strong seismic risk zones", *B. Earthq. Eng.*, **10**(6), 1885-1909.
- Kalantari, A. and Amjadian, M. (2010), "An approximate method for dynamic analysis of skewed highway bridges with continuous rigid deck", *Eng. Struct.*, **32**(9), 2850-2860.
- Amjadian, M. and Kalantari, A. (2012), "Influence of seismic pounding on dynamic response of skewed highway bridges", *15th World Conference on Earthquake Engineering*, Lisbon.
- Ataei, N. and Padgett, J.E (2013), "Limit state capacities for global performance assessment of bridges exposed to hurricane surge and wave", *Struct. Saf.*, **41**, 73-81.
- Bayat, M., Daneshjoo, F. and Nisticò, N. (2015a), "Probabilistic sensitivity analysis of multi-span highway bridges", *Steel Compos. Struct.*, **19**(1), 237-262.
- Bayat, M., Daneshjoo, F. and Nisticò, N. (2015b), "A novel proficient and sufficient intensity measure for probabilistic analysis of skewed highway bridges", *Struct. Eng. Mech.*, **55**(6), 1177-1202.
- Bisadi, V., Head, M. and Gardoni, P. (2011), "Seismic fragility estimates and optimization of retrofitting strategies for reinforced concrete bridges", *Case study of the fabela bridge in Toluca, Mexico, ASCE Structures Congress*, 13-22.
- Boore, D.M., Joyner, W.B. and Fumal, T.E. (1993), "Estimation of response spectra and peak accelerations from western North American earthquakes: an interim report", Open-File Report 93-509, U.S. Geological Survey.
- Choi, E., DesRoches, R. and Nielson, B. (2004), "Seismic fragility of typical bridges in moderate seismic zones", *Eng. Struct.*, **26**(2), 187-199.
- Cimerallo, G.P., Reinhorn, A.M. and Bruneau, M. (2010), "Framework for analytical quantification of disaster resilience", *Eng. Struct.*, **32**(11), 3639-3649.
- Cornell, A.C., Jalayer, F. and Hamburger, R.O. (2002), "Probabilistic basis for 2000 SAC federal emergency management agency steel moment frame guidelines", *J. Struct. Eng.*, **128**(4), 526-532.
- Deepu, S.P., Prajapat. K. and Ray-Chaudhuri. S. (2014), "Seismic vulnerability of skew bridges under bi-directional ground motions", *Eng. Struct.*, **71**(9), 150-160.
- Eads, L., Miranda, E., Krawinkler, H. and Lignos, D. (2013), "An efficient method for estimating the collapse risk of structures in seismic regions", *Earthq. Eng. Struct. D.*, **42**(1), 25-41.
- Elnashai, A.S, Borzi, B. and Vlachos, S. (2004), "Deformation-based vulnerability functions for R/C bridges", *Struct. Eng. Mech.*, **17**(2), 215-244.
- Federal Emergency Management Agency (1999), "Multi-hazard loss estimation methodology, earthquake model", HAZUS99 User's Manual, Washington DC.
- FEMA (2003), HAZUS-MH MR1: Technical Manual, Federal Emergency Management Agency Washington, DC.

- Ghobarah, A. and Tso, W. (1973), "Seismic analysis of skewed highway bridges with intermediate supports", *Earthq. Eng. Struct. D.*, **2**(3), 235-248.
- Hwang, H., Liu, J. and Chiu, Y. (2001), "Seismic fragility analysis of highway bridges", Center for Earthquake Research and Information, University of Memphis, Memphis, Technical Report.
- Kameshwar, S. and Padgett, J.E. (2014), "Multi-hazard risk assessment of highway bridges subjected to earthquake and hurricane hazards," *Eng. Struct.*, **78**(11), 154-166.
- Katsanos, E.I. and Sextos, A.G. (2013), "An integrated software environment for structure-specific earthquake ground motion selection," *Adv. Eng. Soft.*, **58**, 70-85.
- Mackie, K. and Stojadinovic, B. (2003), "Seismic demands for performance-based design of bridges," PEER Report No. 2003/16, Pacific Earthquake Engineering Research Center, University of California, Berkeley CA.
- Maragakis, E.A. and Jennings, P.C. (1987), "Analytical models for the rigid body motions of skew bridges", *Earthq. Eng. Struct. D.*, **15**(8), 923-944.
- Meng, J.Y. and Lui, E.M. (2000), "Seismic analysis and assessment of a skew highway bridge", *Eng. Struct.*, **22**, 1433-1452.
- Nielson, G.B. (2005), "Analytical fragility curves for highway bridges in moderate seismic zones", Georgia Institute of Technology, in partial requirement for the requirement for Doctor of Philosophy.
- Padgett Jamie, E., Nielson Bryant, G. and DesRoches, R. (2008), "Selection of optimal intensity measures in probabilistic seismic demand models of highway bridge portfolios", *Earthq. Eng. Struct. D.*, **37**(5), 711-725.
- Shinozuka, M., Feng, M.Q., Kim, H., Uzawa, T. and Ueda, T. (2001), "Statistical analysis of bridge fragility curves", Unpublished MCEER Technical Report.
- Shinozuka, M., Kim, S.H., Koshiyama S. and Yi, J.H. (2002), "Fragility curves of concrete bridges retrofitted by Column Jacketing", *J. Earthq. Eng. E. Vibr.*, **1**(2), 195-205
- Sung, Y.C. and Su, C.K. (2011), "Time-dependent seismic fragility curves on optimal retrofitting of neutralised reinforced concrete bridges", *Struct Infrastr. E.*, **7**(10), 797-805.
- Tavares, D.H., Padgett, J.E. and Paultre P. (2012), "Fragility curves of typical as-built highway bridges in eastern Canada", *Eng. Struct.*, **40**(9), 107-118.
- Wakefield, R.R., Nazmy, A.S. and Billington, D.P. (1991), "Analysis of seismic failure in skew RC bridge", *J. Struct. Eng.*, **117**(3), 972-986.
- Wright, T., DesRoches, R. and Padgett, J.E. (2011), "Bridge seismic retrofitting practices in the Central and Southeastern United States", *J. Bridge Eng.*, **16**(1), 82-92.
- Yi, J.H., Kim, S.H. and Koshiyama, S. (2007), "PDF interpolation technique for seismic fragility analysis of bridges", *Eng. Struct.*, **29**, 1312-1322.